HHS Public Access

Author manuscript

ACS Biomater Sci Eng. Author manuscript; available in PMC 2019 March 15.

Published in final edited form as:

ACS Biomater Sci Eng. 2015 February 9; 1(2): 110–118. doi:10.1021/ab500060r.

Transforming Growth Factor Beta 3 Modifies Mechanics and Composition of Extracellular Matrix Deposited by Human Trabecular Meshwork Cells

Vijay Krishna Raghunathan[†,‡], **Joshua T. Morgan**[†,‡], **Yow-Ren Chang**[‡], **Darren Weber**[§], **Brett Phinney**[§], **Christopher J Murphy**[‡,⊥], and **Paul Russell**[*,‡]

[‡]Department of Surgical and Radiological Sciences, School of Veterinary Medicine, University of California, Davis, California 95616, United States

[§]UC Davis Genome Center Proteomics Core Facility, University of California, Davis, California 95616, United States

[⊥]Department of Ophthalmology and Vision Sciences, School of Medicine, University of California, Davis, California 95616, United States

Abstract

Pseudoexfoliation syndrome is a systemic disorder of the extracellular matrix (ECM) with ocular manifestations in the form of chronic open angle glaucoma. Elevated levels of TGFβ3 in the aqueous humor of individuals with pseudoexfoliation glaucoma (PEX) have been reported. The influence of TGFβ3 on the biochemical composition and biomechanics of ECM of human trabecular meshwork (HTM) cells was investigated. HTM cells from eye bank donor eyes were isolated, plated on aminosilane functionalized glass substrates and cultured in the presence or absence of 1 ng/mL TGFβ3 for 4 weeks. After incubation, samples were decellularized and decellularization was verified by immunostaining. The mechanics of the remaining ECM that was deposited by the treated or the control cells were measured by atomic force microscopy (AFM). Imaged by AFM, the surface features of the ECM from both sets of samples had a similar roughness/topography (as determined by RMS values) suggesting surface features of the ECM were similar in both cases; however, the ECM from the HTM cells treated with TGFβ3 was between 3- and 5-fold stiffer than that produced by the control HTM cells. Proteins present in the ECM were solubilized and analyzed using liquid chromatography tandem mass spectroscopy (LC-MS/MS). Data indicate that multiple proteins previously reported to be altered in glaucoma were changed in the ECM as a result of the presence of TGFβ3, including inhibitors of the BMP and Wnt signaling pathways. Gremlin1and 4, SERPINE1 and 2, periostin, secreted frizzled related protein (SFRP) 1 and 4, and ANGPTL4 were among those proteins that were overexpressed in the ECM after TGFβ3 treatment.

[*]**Corresponding Author** prussell@ucdavis.edu.

[†]V.K.R. and J.T.M. contributed equally to this work and should be considered as co-first authors

Author Contributions

V.K.R. and J.T.M. designed, planned, and executed the study. P.R. and C.J.M. contributed to design of the study. Y.C. contributed to conducting experiments. D.W. and B.P. performed proteomics on samples. V.K.R., J.T.M., and D.W. performed data analysis. All authors contributed toward preparation of the manuscript.

The authors declare no competing financial interest.

Keywords

extracellular matrix; biomechanics; glaucoma; pseudoexfoliation syndrome; trabecular meshwork; atomic force microscopy

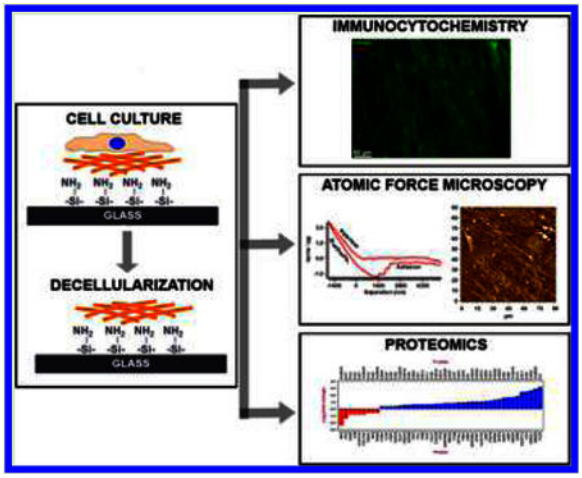

INTRODUCTION

The structural organization and biochemical composition of the extracellular matrix (ECM) has a profound influence on cellular function. Structural proteins of the ECM, such as elastin, collagen, fibronectin, laminin, and fibrillin provide mechanical support for cellular adhesion and migration. The ECM is also composed of a number of matricellular proteins [thrombospondin, tenacin, cysteine-rich angiogenic inducer 61 (CYR61), secreted protein acidic and rich in cysteine (SPARC)], matrix adhesion receptors and molecules (integrins, syndecans), and growth factors (transforming growth factor β (TGFβ), connective tissue growth factor (CTGF)). Although some of these proteins lend no structural support to the ECM, they provide critical functional cues (e.g., growth factor receptor binding, enzymes, cell-adhesion, etc.) to facilitate cellular function and cell−matrix interactions. Enzymes that cleave peptides, such as matrix metalloproteinases (MMPs), and those that form functional cross-links by post-translational modification, such as transglutaminase and lysyl oxidase, are also constituents of the ECM microenvironment. Various nonproteinaceous components [glycosaminoglycans (GAG)] interact with ECM proteins to form chains of carbohydrate rich elements called proteoglycans to facilitate molecular transport, tissue swelling and compressibility. Maintaining the integrity and homeostasis of the ECM is vital for normal healthy tissue function. Dysregulation of the ultrastructure, protein or GAG composition, and enzymatic activity of the matrix all lead to remodeling of the ECM, deposition of plaque-like material, and to the progression and maintenance of the diseased state. Therefore, understanding the dynamic bidirectional interaction between cells and their matrix microenvironment is vital in understanding the homeostasis of the cell.

Pseudoexfoliation syndrome is a systemic disorder of the ECM that affects the eye and other organs. The ocular manifestations include the occurrence of small white deposits of fibrillar material in the anterior segment, elevated intraocular pressure (IOP), chronic open-angle

glaucoma, and cataract.[1,2] Resistance to aqueous humor outflow by the trabecular meshwork (TM) is one of the primary causes for the increase in intraocular pressure (IOP). In PEX, whether this increased resistance is due to the exfoliation material or altered tissue morphology or composition of the ECM and/or a combination of both is not known. Although the biomechanical characterization of normal and POAG TM has previously been reported by our group and others,[3−5] the difficulty in obtaining human tissues makes it challenging to characterize the mechanics in all types of glaucoma. Also, currently there is a paucity of in vivo models for studying cell-ECM dynamics in PEX. However, there is consensus that a number of proteins of the ECM and aqueous humor are altered in PEX patients.

The protein content in the aqueous humor of patients with PEX is remarkably higher than age-matched control patients, or in patients with cataract, or individuals with other primary or secondary open angle glaucoma.[6−9] Transforming growth factor β (TGFβ) superfamily of proteins (TGFβ1, TGFβ2, and TGFβ3) play an essential role in cellular signaling and ECM remodeling and is elevated in the aqueous humor of patients with glaucoma.[10−14] While most studies document elevated levels of TGFβ2 in open angle glaucoma and TGFβ1 in PEX, Yoneda et al. demonstrated that TGFβ3 was the most significantly elevated (>10-fold) protein from the TGFβ family in aqueous humor of patients with PEX.[14] That TGFβ1 and TGFβ2 can significantly modulate ECM expressing genes and/or modulate IOP in TM is well established.[15−18] Surprisingly little is known about the role of TGFβ3 in regulating IOP changes or in modulating the biophysical properties and biochemical composition of TM ECM. Here, we report the effect of TGFβ3 on the composition and mechanical properties of ECM derived from human trabecular meshwork (HTM) cells in vitro and discuss the relevancy of findings in the context of ECM changes in TM function.

EXPERIMENTAL SECTION

Isolation and Culture of HTM Cells.

Primary HTM cells were isolated from donor corneoscleral rims (Saving Sight, Columbia, MO) as described previously.[19] All experiments involving human tissue/cells were performed in compliance with the Declaration of Helsinki. HTM cells isolated from three donors were used for each experiment and were routinely maintained in Dulbecco's Modified Eagle Medium/Nutrient Mixture F-12 (50:50; DMEM/F-12) supplemented with 10% fetal bovine serum (FBS), and 1% penicillin/streptomycin/fungizone (Life Technologies, Carlsbad, CA). Cells were used between passages three and seven for all experiments. The verification of all cultures as HTM cells was determined by response to dexamethasone treatment by upregulating myocilin expression.

Treatment with Transforming Growth Factor Beta-3 (TGFβ3).

Cells (25 000 cells/cm^2) were cultured on amino-silane modified glass coverslips (for ECM mechanics) or glass slides (for ECM proteomics). Briefly, glass substrates were incubated with 3-aminopropyl trimethoxysilane overnight under vacuum. Silanized coverslips were heat treated at 200 °C for 20 min. Freshly silanized substrates were used for all experiments. Primary HTM cells were seeded on these silanized substrates as described above. Cells were

treated with TGFβ3 (1 ng/mL) twice a week for 4 weeks. The four week time point was chosen to allow sufficient time for matrix deposition and remodeling.

Preparation of Decellularized Matrices.

Following treatment with TGFβ3 or vehicle (phosphate buffered saline), cells were washed twice in Hank's buffered saline solution (HBSS), and then serially washed five times with 20 mM NH_4OH and 0.05% Triton X-100 to rid the matrix of all cells. The matrix was subsequently washed five times in HBSS and decellularization was confirmed by immunocytochemistry. A schematic for the generation of these matrices is illustrated in Figure 1.

Immunocytochemistry.

Decellularization was confirmed by immunocytochemistry. Briefly, cell derived matrices were washed gently yet thoroughly in HBSS, fixed in 4% formaldehyde for 20 min. The matrix was then labeled for pan-collagen (1:1000 dilution, Abcam, MA), F-actin (1:500 dilution, AlexaFluor-568 conjugated Phalloidin, Life Technologies, CA), and counterstained with DAPI (5 ng/mL final concentration, Life Technologies, CA) for the presence of nuclear material. The samples were then imaged using a Zeiss 200 M inverted epifluorescence microscope (Carl Zeiss, Germany).

ECM Characterization by Proteomics.

Following 4 weeks of treatment with vehicle (PBS) or 1 ng/mL TGFβ3, samples were decellularized as described above. Subsequently, they were rinsed five times in HBSS and incubated for 3 min with 150 μL of ECM extraction buffer comprising 4 M guanidine hydrochloride and 10 mM dithiothreitol (DTT) in deionized water (dH_2O). Samples were scraped into a microfuge tube, vortexed for 2 min to ensure dissolution of the ECM, and used for proteomic analysis.

Sample Digestion.

Samples were precipitated using the ProteoExtract protein precipitation kit (EMD Millipore, MA, USA). The resulting protein pellet was solubilized in 100 μL of 6 M urea in 50 mM ammonium bicarbonate (AMBIC). Dithiothreitol (DTT) was added to a final concentration of 5 mM and samples were incubated for 30 min at 37 °C. Next, 20 mM iodoacetamide (IAA) was added to a final concentration of 15 mM and incubated for 30 min at room temperature, followed by the addition of 20 μL of 200 mM DTT to quench the IAA reaction. Lys-C/trypsin (Promega, USA) was next added in a 1:25 ratio (enzyme:protein) and incubated at 37 °C for 4 h. Samples were then diluted to <1 M urea by the addition of 50 mM AMBIC and digested overnight at 37 °C. The following day, samples were desalted using C18 Macro Spin columns (Nest Group) and dried down by vacuum centrifugation.

LC-MS/MS Analysis.

LC separation was done on a Waters Nano Acquity UHPLC (Waters Corporation, MA) with a Proxeon nanospray source. The digested peptides were reconstituted in 2% acetonitrile/ 0.1% trifluoroacetic acid and roughly 3 μg (estimated by A280 levels using NanoDrop, DE,

USA) of each sample was loaded onto a 100 μm × 25 mm Magic C18 100 Å 5U reverse phase trap where they were desalted online before being separated on a 75 μm × 150 mm Magic C18 200 Å 3U reverse phase column. Peptides were eluted using a gradient of 0.1% formic acid (A) and 100% acetonitrile (B) with a flow rate of 300 nL/min. A 120 min gradient was ran with 5 to 35% B over 100 min, 35 to 80% B over 8 min, 80% B for 1 min, 80 to 5% B over 1 min, and finally held at 5% B for 10 min. Each of the gradients was followed by a 1 h column wash.

Mass spectra were collected on an Orbitrap Q Exactive Plus mass spectrometer (Thermo Fisher Scientific, CA) in a data-dependent mode with one MS precursor scan followed by 15 MS/MS scans. A dynamic exclusion of 15 s was used. MS spectra were acquired with a resolution of 70,000 and a target of 1×10^6 ions or a maximum injection time of 30 ms. MS/MS spectra were acquired with a resolution of 17 500 and a target of 5×10^4 ions or a maximum injection time of 50 ms. Peptide fragmentation was performed using higher-energy collision dissociation (HCD) with a normalized collision energy (NCE) value of 27. Unassigned charge states as well as +1 and ions >+5 were excluded from MS/MS fragmentation.

Data Analysis.

Database Searching.—Tandem mass spectra were extracted and charge states were deconvoluted and deisotoped. All MS/MS samples were analyzed using X! Tandem (The GPM, thegpm.org; version X! Tandem Sledgehammer (2013.09.01.1)). X! Tandem was set up to search the Uniprot Homo sapiens database (July 2014, 68370 entries) plus an equal number of reverse sequences and 60 common nonhuman laboratory contaminant proteins. X! Tandem was searched with a fragment ion mass tolerance of 20 PPM and a parent ion tolerance of 20 PPM. Carbamidomethyl of cysteine was specified in X! Tandem as a fixed modification. Glu → pyro-Glu of the N-terminus, ammonia-loss of the N-terminus, gln → pyro-Glu of the N-terminus, deamidation of asparagine and glutamine, oxidation of methionine and tryptophan, and dioxidation of methionine and tryptophan were specified in X! Tandem as variable modifications.

Criteria for Protein Identification.—Scaffold (version Scaffold_4.3.0, Proteome Software Inc., Portland, OR) was used to validate MS/MS-based peptide and protein identifications. Peptide identifications were accepted if they could be established at a 99.0% probability by the Scaffold Local FDR algorithm this corresponded to a 0.23% spectra decoy FDR and a 4% protein decoy FDR with 1 identified peptide per protein. Protein probabilities were assigned by the Protein Prophet algorithm.[20] Proteins that contained similar peptides and could not be differentiated based on MS/MS analysis alone were grouped to satisfy the principles of parsimony. Proteins sharing significant peptide homology were grouped into clusters.

Contact Mechanics.

The mechanical properties of cell derived ECM were determined using the MFP-3D Bio AFM (Asylum Research, Santa Barbara, CA) coupled with a Zeiss Axio Observer inverted microscope (Carl Zeiss, Thornwood, NY). Force curves were obtained using silicon nitride

cantilevers (PNP-TR-50, nominal spring constant (κ) of 0.32 N/m and half angle opening of 35°, NanoAndMore, Lady's Island, SC) modified by incorporation of a borosilicate bead (nominal radius, R = 5 μm, ThermoScientific, Fremont, CA, USA) at the free end of the cantilever; These colloidal probes were calibrated for deflection inverse optical lever sensitivity (Defl InvOLS) by indentation in HBSS on glass and then the actual spring constant of the cantilever was determined by the thermal method using the Asylum Research software. All samples were equilibrated in HBSS for 30 min prior to obtaining measurements. For all samples, five force curves were obtained from at least seven different positions.

Elastic modulus of each sample was obtained by fitting indentation force vs indentation depth of the sample with an overlay of the theoretical force based on the geometry-appropriate Hertz model for spherical tip (eq 1) as described previously.[21−23]

$$F = \frac{4}{3}\frac{E}{1-\nu^2}\delta^{3/2}R^{1/2} \quad (1)$$

where F is force applied by the indenter, E is Young's modulus, v is Poisson's ratio, δ is indentation depth, and R is radius of the tip. All biological samples were assumed as incompressible materials because of their high water content and therefore the Poisson's ratio was assumed to be 0.5.[24−28] Determining the accurate indentation depth across which the biological sample behaves as a linear-elastic material is difficult from the F vs δ curves. Thus, the elastic regime of a viscoeleastic tissue, where E is constant over a restricted indentation depth, was determined from a plot of E versus δ values.[29]

Imaging the ECM.

Immediately after obtaining force measurements on the decellularized ECM samples, they were rinsed thoroughly in dH_2O and air-dried overnight at 37 °C. ECM samples were then imaged in contact mode using an AC240TS cantilever (nominal κ = 1.5 N/m; NanoAndMore) at 500 pN applied force and 0.3 Hz.

Statistical Analysis.

All mechanics data are represented as box and whisker plots to demonstrate data distribution. Statistical comparison of mechanics between vehicle and TGFβ3 treated cells was done using Mann−Whitney U-test and results are indicated in the plots. Shotgun proteomics data were analyzed using Scaffold Viewer (Proteome Software Inc., OR). Using the built-in features of the software normalized total spectral counts from the three different cell cultures were compared for fold-change between the control and TGFβ3 samples. The relative abundance between the two groups was compared using Fisher's exact test.[30]

RESULTS

HTM cells from all three donors were cultured for 4 weeks in the presence or absence of 1 ng/mL TGFβ3 to allow for deposition of ECM. Decellularization after treatment with NH_4OH was confirmed by immunocytochemistry (Figure 2). All ECM samples stained

positively for pan-collagen simultaneously being devoid of cytoskeletal or nuclear components as evidenced by a lack of F-actin or DAPI staining, respectively. Analysis of force vs indentation curves to determine the elastic moduli of HTM cell derived ECM revealed that TGFβ3 treated cells deposited a significantly stiffer ECM compared with control cultures (Figure 3). The elastic moduli for ECM derived from control cells ranged between 0.17−0.34 kPa with a mean of 0.26 ± 0.12 kPa (mean ± standard deviation), whereas those derived after TGFβ3 treatment were between 0.90 and 1.07 kPa with a mean of 0.98 ± 0.13 kPa (mean ± standard deviation).

Concurrent with changes to the elastic moduli of the ECM, morphological (topographical) alterations to the deposited ECM were assessed by imaging using the AFM. Surface topography of the ECM deposited by TGFβ3 treated cells appeared similar to control cells. Quantitative analysis of 4 random locations revealed that the root-mean-square (RMS) of control-cell-derived ECM was 70 ± 18.31 nm (mean ± standard deviation) and that of TGFβ3-derived matrix was 97.69 ± 7.01 nm (mean ± standard deviation) (Figure 4). Although TGFb3 treated cells deposited a stiffer matrix, no statistically significant differences were observed between the two groups with regards to surface topography of the ECM as determined by RMS values. Further studies are required to determine subtle alterations in the three-dimensional ultra-strcutre of ECM between the two groups.

Biochemical composition of ECM derived from control and TGFβ3-treated cells were determined by performing mass spectrometry and subsequent analyses of spectral counts; 4935 proteins were identified. Only proteins that were altered by at least 1.3-fold with p-values less than 0.05 (Fisher's exact test) in all three cell cultures for either control or TGFβ3-treated samples were used for functional analysis (Figure 5 and Table 1). Of specific interest, secreted frizzled-related protein 1 and 4 (SFRP1 and SFRP4), plasminogen activator inhibitor type 1 (SERPINE1), angiopoietin-like 4 (ANGPTL4), periostin (POSTN), gremlin 1 (GREM1), and fibroblast growth factor 5 (FGF5) were overexpressed greater than 2-fold, whereas interalpha-trypsin inhibitor heavy chain 3 (ITIH3) and melanotransferrin (MFI2) were decreased 2-fold in the ECM derived from TGFβ3 treated cells (Table 2). The data set from this study can be downloaded from the MassIVE proteomics repository (MassIVE ID# MSV000078897) at ftp://MSV000078897@massive.ucsd.edu.

DISCUSSION

The deposition and turnover of ECM in the TM is critical to understanding regulation of outflow facility, intraocular pressure and the mechanobiology of glaucoma. In PEX, elevated IOP has been largely attributed to the blockage of the TM by exfoliation material;[31] however, the extent to which TM cell dysfunction contributes to ocular hypertension is less known. The precise extent to which either of these contributes to the inhibition of outflow facility is poorly understood. Although a number of studies indicate a significant involvement of the TGFβ superfamily of proteins in this disease,[12,14,32−37] most have concentrated on the role of TGFβ1 and 2. Little is known of the effects of TGFβ3 on ECM remodeling in the TM, although its ability to stimulate ECM deposition by corneal keratocytes has been previously demonstrated.[38]

Here, we demonstrate that chronic TGFβ3 treatment significantly alters the biophysical properties and biochemical composition of matrix proteins deposited by TM cells. Tellingly, the ECM deposited by TGFβ3 treated cells was three-to-5-fold stiffer (greater elastic modulus) than that deposited by control HTM cells. Our group and others have demonstrated that substrate stiffness can alter cytoskeletal organization and protein/gene expression in various cell types including HTM cells.[39–44] Although most studies performed to investigate the short-term effect of substratum stiffness employ polymeric hydrogels or collagen scaffolds/gels, to the best of the authors' knowledge, there are no studies that have investigated the effects of altered biomechanical properties of cell-derived matrices on cellular function. The methodology described here to generate TM cell-derived matrices provides a novel and potentially important tool for studying HTM cell− ECM interactions during differentiation, mechanotransduction, and ECM remodeling.

With TGFβ3 treatment, not only was the ECM stiffer, but a number of proteins in the extracellular milieu pertinent to HTM function were significantly altered. Most notably, secreted frizzled related protein, periostin, gremlin, angiopoietin like protein, and plasminogen activator inhibitor protein 1 were all overexpressed 2-fold or greater in ECM deposited by TGFβ3-treated cells. Gremlin, an antagonist of bone morphogenic protein signaling (BMP), is reported to be overexpressed in fibrosis and in epithelial-mesenchymal transition (EMT).[45–48] Of particular importance, gremlin was reported to inhibit BMP-4 activity, thereby promoting TGFβ2 signaling in cultured HTM cells and was shown to increase outflow resistance in perfusion cultured human eye.[49] Although it has been speculated that gremlin may exaggerate the pro-fibrotic effects of TGFβ1 and 2 in the TM, our data suggest that TGFβ3 may participate in increasing gremlin expression in the extracellular microenvironment, thus resulting in adverse TGFβ signaling feedback for remodeling the TM ECM.

Angiopoietin-like (ANGPTL) proteins are a family of glycoproteins that have long been known to mediate glucose and lipid metabolism and inflammation. The most widely reported protein of this family in glaucoma is ANGPTL-7, which is known to be overexpressed in aqueous humor of glaucomatous patients[50] and in TM cells treated with dexamethasone and TGFβ2.[18,51–53] TGFβ3 stimulated expression of ANGPTL4 has previously been reported during chondrogenic differentiation of mesenchymal stem cells.[54] Little is known of the role of ANGPTL4 in the TM. ANGPTL4 in its active form can bind to heparin sulfate proteoglycans, fibronectin, and vitronectin, thus delaying their degradation by matrix metalloproteinases (MMPs).[55,56] Delayed degradation of ECM proteins can potentially impact the cell−ECM interactions, such as cell spreading and migration, via altered integrin signaling, focal adhesions, and cytoskeletal remodelling. Specifically, ANGPTL4 is known to directly interact with integrins β1 and β5.[57] The direct interaction of integrin $\alpha_v\beta_1$ with fibronectin allows for a stronger force to be exerted by cells on rigid matrices.[58] The extent to which ANGPTL4 may compete with fibronectin to bind to β1 integrins in HTM cells or its subsequent impact on cell−ECM interaction is not known at this time.

Another ECM protein that can associate with TGFβ, tenascin, and fibronectin is periostin. Overexpressed in the ECM deposited by TGFβ3 treated cells, periostin is a critical

matricellular protein whose expression levels strongly correlate with calcification, collagen deposition, collagen cross-linking, and fibrillogenesis.[59−62] Cross-linking of collagen would alter biomechanical properties resulting in a stiffer ECM. Indeed, perisotin was up-regulated in TM cells subjected to mechanical stretch and in the optic nerve head of rat models with elevated IOP.[63,64] Another protein that accumulates with collagen fibers and is a positive regulator of fibrosis is the extracellular isoform of adipocyte enhancer binding protein 1 (AEBP1).[65−67] AEBP-1 was also found to be overexpressed with TGFβ3 stimulated HTM derived ECM.

Both ex vivo and *in vivo* studies have demonstrated that treatment of TM cells with the Wnt antagonist, secreted frizzled related protein (SFRP1) elevates IOP and reduces outflow facility.[68] We have previously shown in vitro that HTM cells cultured on substrates whose stiffness mimics glaucoma-tous TM had elevated SFRP1 expression.[39] In this study, we report that chronic TGFβ3 treatment resulted in elevated secretion of SFRP1 and 4 by HTM cells demonstrating a link between Wnt inhibition, TGFβ signaling, and stiffness. The extended presence of Wnt inhibitors in the extracellular milieu may perturb Wnt signaling, a major pathway implicated in glaucoma, in HTM cells. The co-occurrence of these factors suggests complex and redundant interactions between the molecules implicated in the onset and progression of glaucoma, where activation of a single signaling process leads to the induction of other factors known to independently induce glaucoma.

Although a number of proteins could potentially result in Wnt antagonism or collagen cross-linking, or for those promoting fibrosis that were overexpressed, the most markedly inhibited proteins were inter-α-trypsin inhibitor heavy chain 3 (ITIH3) and melanotransferrin (MFI). ITIH3 is most recognized to interact with hyaluronan, a nonsulfated glycosaminoglycan, to stabilize the matrix.[69,70] Hylauronan is a major component of the TM ECM; but a role of ITIH in glaucoma, remodeling of the TM ECM or in pseudoexfoliation has not been previously reported. Melanotransferrin (MFI), a glycosylated protein, is known to activate plasminogen activator (PA) and result in cell detachment.[71,72] Inhibited expression of MFI combined with overexpression of plasminogen activator inhibitor 1 (PAI-1/SERPINE1) in ECM of TGFβ3-treated HTM cells suggests the likelihood of stronger cell attachment. In aggregate, these changes in protein expression identify new mechanistic targets for research in PEX, and further research will be required to understand their contribution to the cellular and extracellular milieu of the TM.

CONCLUSION

The results presented in this study, taken in aggregate, suggest that TGFβ3 may play a significant role in modulating the biomechanics and biochemical composition of ECM deposited by TM cells. Specifically, overexpression of proteins that are markers of fibrosis, calcification, enhancers of cell−substratum adhesion and force dynamics, and inhibitors of matrix degradation indicates that TGFβ3 signaling in the TM may be a critical contributor to the increased resistance to outflow facility of the TM and the elevation of IOP in PEX.

ACKNOWLEDGMENTS

The authors thank Ms. Linda Huang for technical assistance.

Funding

This study was funded by grants from the National Institutes of Health R01EY019475, P30EY12576, and unrestricted funds from Research to Prevent Blindness.

REFERENCES

(1). Ritch R; Schlötzer-Schrehardt U Exfoliation Syndrome. Surv. Ophthalmol 2001, 45, 265–315. [PubMed: 11166342]

(2). Schlötzer-Schrehardt U; von der Mark K; Sakai LY; Naumann GO Increased extracellular deposition of fibrillin-containing fibrils in pseudoexfoliation syndrome. Invest. Ophthalmol. Vis. Sci 1997, 38, 970–984. [PubMed: 9112993]

(3). Last JA; Pan T; Ding Y; Reilly CM; Keller K; Acott TS; Fautsch MP; Murphy CJ; Russell P Elastic modulus determination of normal and glaucomatous human trabecular meshwork. Invest. Ophthalmol. Vis. Sci 2011, 52, 2147–2152. [PubMed: 21220561]

(4). Camras LJ; Stamer WD; Epstein D; Gonzalez P; Yuan F Circumferential Tensile Stiffness of Glaucomatous Trabecular Mesh-work. Invest. Ophthalmol. Vis. Sci 2014, 55, 814–823. [PubMed: 24408980]

(5). Camras LJ; Stamer WD; Epstein D; Gonzalez P; Yuan F Differential Effects of Trabecular Meshwork Stiffness on Outflow Facility in Normal Human and Porcine Eyes. Invest. Ophthalmol. Vis. Sci 2012, 53, 5242–5250. [PubMed: 22786899]

(6). Koliakos GG; Konstas AG; Dimitrakoulias N; Triantos A; Kardasopoulos A; Dimitriadou A; Trakatellis AC Possible role of transferrin in exfoliation syndrome. Acta Ophthalmol. Scand 1996, 74, 155–159. [PubMed: 8739681]

(7). Küchle M; Ho TS; Nguyen NX; Hannappel E; Naumann GO Protein quantification and electrophoresis in aqueous humor of pseudoexfoliation eyes. Invest. Ophthalmol. Vis. Sci 1994, 35, 748–752. [PubMed: 8113026]

(8). Küchle M; Nguyen NX; Hannappel E; Naumann GO The blood-aqueous barrier in eyes with pseudoexfoliation syndrome. Ophthalmic Res 1995, 27 (Suppl 1), 136–142.

(9). Küchle M; Nguyen NX; Horn F; Naumann GO Quantitative assessment of aqueous flare and aqueous ‘cells’ in pseudoexfoliation syndrome. Acta Ophthalmol. (Copenh.) 1992, 70, 201–208. [PubMed: 1609568]

(10). Koliakos GG; Schlotzer-Schrehardt U; Konstas AG; Bufidis T; Georgiadis N; Dimitriadou A Transforming and insulin-like growth factors in the aqueous humour of patients with exfoliation syndrome. Graefes Arch. Clin. Exp. Ophthalmol 2001, 239, 482–487. [PubMed: 11521691]

(11). Tripathi RC; Li J; Chan WA; Tripathi BJ Aqueous humor in glaucomatous eyes contains an increased level of TGF-β2. Exp. Eye Res 1994, 59, 723–728. [PubMed: 7698265]

(12). Picht G; Welge-Luessen U; Grehn F; Lutjen-Drecoll E Transforming growth factor beta 2 levels in the aqueous humor in different types of glaucoma and the relation to filtering bleb development. Graefes Arch. Clin. Exp. Ophthalmol 2001, 239, 199–207. [PubMed: 11405069]

(13). Prendes MA; Harris A; Wirostko BM; Gerber AL; Siesky B The role of transforming growth factor β in glaucoma and the therapeutic implications. Br. J. Ophthalmol 2013, 97, 680–686. [PubMed: 23322881]

(14). Yoneda K; Nakano M; Mori K; Kinoshita S; Tashiro K Disease-related quantitation of TGF-beta3 in human aqueous humor. Growth Factors 2007, 25, 160–167. [PubMed: 18049952]

(15). Fitzgerald AM; Benz C; Clark AF; Wordinger RJ The effects of transforming growth factor-β2 on the expression of follistatin and activin A in normal and glaucomatous human trabecular meshwork cells and tissues. Invest. Ophthalmol. Vis. Sci 2012, 53, 7358–7369. [PubMed: 23010638]

(16). Sethi A; Jain A; Zode GS; Wordinger RJ; Clark AF Role of TGFβ/Smad Signaling in Gremlin Induction of Human Trabecular Meshwork Extracellular Matrix Proteins. Invest. Ophthalmol. Vis. Sci 2011, 52, 5251–5259. [PubMed: 21642622]

(17). Sethi A; Mao W; Wordinger RJ; Clark AF Transforming Growth Factor–β Induces Extracellular Matrix Protein Cross-Linking Lysyl Oxidase (LOX) Genes in Human Trabecular Meshwork Cells. Invest. Ophthalmol. Vis. Sci 2011, 52, 5240–5250. [PubMed: 21546528]

(18). Zhao X; Ramsey KE; Stephan DA; Russell P Gene and Protein Expression Changes in Human Trabecular Meshwork Cells Treated with Transforming Growth Factor-β. Invest. Ophthalmol. Vis. Sci 2004, 45, 4023–4034. [PubMed: 15505052]

(19). Morgan JT; Wood JA; Walker NJ; Raghunathan VK; Borjesson DL; Murphy CJ; Russell P Human trabecular meshwork cells exhibit several characteristics of, but are distinct from, adipose-derived mesenchymal stem cells. J. Ocul. Pharmacol. Ther 2014, 30, 254–266. [PubMed: 24456002]

(20). Nesvizhskii AI; Keller A; Kolker E; Aebersold R A statistical model for identifying proteins by tandem mass spectrometry. Anal. Chem 2003, 75, 4646–4658. [PubMed: 14632076]

(21). Thomasy SM; Raghunathan VK; Winkler M; Reilly CM; Sadeli AR; Russell P; Jester JV; Murphy CJ Elastic modulus and collagen organization of the rabbit cornea: epithelium to endothelium. Acta Biomater 2014, 10, 785–791. [PubMed: 24084333]

(22). McKee CT; Raghunathan VK; Nealey PF; Russell P; Murphy CJ Topographic modulation of the orientation and shape of cell nuclei and their influence on the measured elastic modulus of epithelial cells. Biophys. J 2011, 101, 2139–2146. [PubMed: 22067151]

(23). McKee CT; Wood JA; Shah NM; Fischer ME; Reilly CM; Murphy CJ; Russell P The effect of biophysical attributes of the ocular trabecular meshwork associated with glaucoma on the cell response to therapeutic agents. Biomaterials 2011, 32, 2417–2423. [PubMed: 21220171]

(24). Anseth KS; Bowman CN; Brannon-Peppas L Mechanical properties of hydrogels and their experimental determination. Biomaterials 1996, 17, 1647–1657. [PubMed: 8866026]

(25). Dimitriadis EK; Horkay F; Maresca J; Kachar B; Chadwick RS Determination of Elastic Moduli of Thin Layers of Soft Material Using the Atomic Force Microscope. Biophys. J 2002, 82, 2798–2810. [PubMed: 11964265]

(26). Ahearne M; Yang Y; El Haj AJ; Then KY; Liu KK Characterizing the viscoelastic properties of thin hydrogel-based constructs for tissue engineering applications. J. R.Soc 2005, 2, 455–463.

(27). Vinckier A; Semenza G Measuring elasticity of biological materials by atomic force microscopy. FEBS Lett 1998, 430, 12–16. [PubMed: 9678586]

(28). Hermann LR Elasticity equations for incompressible and nearly incompressible materials by a variational theorem. AIAA J 1965, 3, 1896–1900.

(29). Mahaffy RE; Shih CK; MacKintosh FC; Kas J Scanning probe-based frequency-dependent microrheology of polymer gels and biological cells. Phys. Rev. Lett 2000, 85, 880–883. [PubMed: 10991422]

(30). Zhang B; VerBerkmoes NC; Langston MA; Uberbacher E; Hettich RL; Samatova NF Detecting differential and correlated protein expression in label-free shotgun proteomics. J. Proteome Res 2006, 5, 2909–2918. [PubMed: 17081042]

(31). Jacobi PC; Krieglstein GK Trabecular aspiration. A new mode to treat pseudoexfoliation glaucoma. Invest. Ophthalmol. Vis. Sci 1995, 36, 2270–2276. [PubMed: 7558721]

(32). Jelodari-Mamaghani S; Haji-Seyed-Javadi R; Suri F; Nilforushan N; Yazdani S; Kamyab K; Elahi E Contribution of the latent transforming growth factor-β binding protein 2 gene to etiology of primary open angle glaucoma and pseudoexfoliation syndrome. Mol. Vis 2013, 19, 333–347. [PubMed: 23401661]

(33). Djordjevic-Jocic J; Zlatanovic G; Veselinovic D; Jovanovic P; Djordjevic V; Zvezdanovic L; Stankovic-Babic G; Vujanovic M; Cekic S; Zenkel M; Schlotzer-Schrehardt U Transforming growth factor beta1, matrix-metalloproteinase-2 and its tissue inhibitor in patients with pseudoexfoliation glaucoma/syndrome. Vojnosanit. Pregl 2012, 69, 231–236. [PubMed: 22624408]

(34). Kara S; Yildirim N; Ozer A; Colak O; Sahin A Matrix metalloproteinase-2, tissue inhibitor of matrix metalloproteinase-2, and transforming growth factor beta 1 in the aqueous humor and serum of patients with pseudoexfoliation syndrome. Clin. Ophthalmol 2014, 8, 305–309. [PubMed: 24511224]

(35). Kottler UB; Junemann AG; Aigner T; Zenkel M; Rummelt C; Schlotzer-Schrehardt U Comparative effects of TGF-beta 1 and TGF-beta 2 on extracellular matrix production, proliferation, migration, and collagen contraction of human Tenon's capsule fibroblasts in

pseudoexfoliation and primary open-angle glaucoma. Exp. Eye Res 2005, 80, 121–134. [PubMed: 15652533]

(36). Schlötzer-Schrehardt U; Küchle M; Hofmann-Rummelt C; Kaiser A; Kirchner T [Latent TGF-beta 1 binding protein (LTBP-1); a new marker for intra-and extraocular PEX deposits]. Klin Monbl Augenheilkd 2000, 216, 412–419. [PubMed: 10919121]

(37). Schlotzer-Schrehardt U; Zenkel M; Kuchle M; Sakai LY; Naumann GO Role of transforming growth factor-beta1 and its latent form binding protein in pseudoexfoliation syndrome. Exp. Eye Res 2001, 73, 765–780. [PubMed: 11846508]

(38). Karamichos D; Rich CB; Zareian R; Hutcheon AE; Ruberti JW; Trinkaus-Randall V; Zieske JD TGF-beta3 Stimulates Stromal Matrix Assembly by Human Corneal Keratocyte-Like Cells. Invest. Ophthalmol. Vis. Sci 2013, 54, 6612–6619. [PubMed: 24022012]

(39). Raghunathan VK; Morgan JT; Dreier B; Reilly CM; Thomasy SM; Wood JA; Ly I; Tuyen BC; Hughbanks M; Murphy CJ; Russell P Role of substratum stiffness in modulating genes associated with extracellular matrix and mechanotransducers YAP and TAZ. Invest. Ophthalmol. Vis. Sci 2013, 54, 378–386. [PubMed: 23258147]

(40). Thomasy SM; Morgan JT; Wood JA; Murphy CJ; Russell P Substratum stiffness and latrunculin B modulate the gene expression of the mechanotransducers YAP and TAZ in human trabecular meshwork cells. Exp. Eye Res 2013, 113, 66–73. [PubMed: 23727052]

(41). Thomasy SM; Wood JA; Kass PH; Murphy CJ; Russell P Substratum stiffness and latrunculin B regulate matrix gene and protein expression in human trabecular meshwork cells. Invest. Ophthalmol. Vis. Sci 2012, 53, 952–958. [PubMed: 22247475]

(42). Han H; Wecker T; Grehn F; Schlunck G Elasticity-dependent modulation of TGF-beta responses in human trabecular meshwork cells. Invest. Ophthalmol. Vis. Sci 2011, 52, 2889–2896. [PubMed: 21282571]

(43). Schlunck G; Han H; Wecker T; Kampik D; Meyer-ter-Vehn T; Grehn F Substrate Rigidity Modulates Cell–Matrix Interactions and Protein Expression in Human Trabecular Meshwork Cells. Invest. Ophthalmol. Vis. Sci 2008, 49, 262–269. [PubMed: 18172101]

(44). Wecker T; Han H; Kneitz S; Grehn F; Schlunck G Influence of Extracellular Matrix Stiffness on Micro-RNA Expression in Human Trabecular Meshwork Cells. Biophys. J 2014, 106, 595a DOI: 10.1016/j.bpj.2013.11.3293.

(45). Koli K; Myllarniemi M; Vuorinen K; Salmenkivi K; Ryynanen MJ; Kinnula VL; Keski-Oja J Bone morphogenetic protein-4 inhibitor gremlin is overexpressed in idiopathic pulmonary fibrosis. Am. J. Pathol 2006, 169, 61–71. [PubMed: 16816361]

(46). Myllarniemi M; Lindholm P; Ryynanen MJ; Kliment CR; Salmenkivi K; Keski-Oja J; Kinnula VL; Oury TD; Koli K Gremlin-mediated decrease in bone morphogenetic protein signaling promotes pulmonary fibrosis. Am. J. Respir. Crit. Care Med 2008, 177, 321–329. [PubMed: 17975199]

(47). Carvajal G; Droguett A; Burgos M; Aros C; Ardiles L; Flores C; Carpio D; Ruiz-Ortega M; Egido J; Mezzano S Gremlin: a novel mediator of epithelial mesenchymal transition and fibrosis in chronic allograft nephropathy. Transplant. Proc 2008, 40, 734–739. [PubMed: 18455002]

(48). Lee H; O'Meara SJ; O'Brien C; Kane R The role of gremlin, a BMP antagonist, and epithelial-to-mesenchymal transition in proliferative vitreoretinopathy. Invest. Ophthalmol. Vis. Sci 2007, 48, 4291–4299. [PubMed: 17724219]

(49). Wordinger RJ; Fleenor DL; Hellberg PE; Pang IH; Tovar TO; Zode GS; Fuller JA; Clark AF Effects of TGF-beta2, BMP-4, and gremlin in the trabecular meshwork: implications for glaucoma. Invest. Ophthalmol. Vis. Sci 2007, 48, 1191–1200. [PubMed: 17325163]

(50). Kuchtey J; Kallberg ME; Gelatt KN; Rinkoski T; Komaromy AM; Kuchtey RW Angiopoietin-like 7 secretion is induced by glaucoma stimuli and its concentration is elevated in glaucomatous aqueous humor. Invest. Ophthalmol. Vis. Sci 2008, 49, 3438–3448. [PubMed: 18421092]

(51). Gonzalez P; Epstein DL; Borras T Characterization of Gene Expression in Human Trabecular Meshwork Using Single-Pass Sequencing of *1060* Clones. Invest. Ophthalmol. Vis. Sci 2000, 41, 3678–3693. [PubMed: 11053263]

(52). Tomarev SI; Wistow G; Raymond V; Dubois S; Malyukova I Gene Expression Profile of the Human Trabecular Meshwork: NEIBank Sequence Tag Analysis. Invest. Ophthalmol. Vis. Sci 2003, 44, 2588–2596. [PubMed: 12766061]

(53). Rozsa FW; Reed DM; Scott KM; Pawar H; Moroi SE; Kijek TG; Krafchak CM; Othman MI; Vollrath D; Elner VM; Richards JE Gene expression profile of human trabecular meshwork cells in response to long-term dexamethasone exposure. Mol. Vis 2006, 12, 125–141. [PubMed: 16541013]

(54). Mathieu M; Iampietro M; Chuchana P; Guerit D; Djouad F; Noel D; Jorgensen C Involvement of angiopoietin-like 4 in matrix remodeling during chondrogenic differentiation of mesenchymal stem cells. J. Biol. Chem 2014, 289, 8402–8412. [PubMed: 24505142]

(55). Goh YY; Pal M; Chong HC; Zhu P; Tan MJ; Punugu L; Tan CK; Huang R-L; Sze SK; Tang MBY; Ding JL; Kersten S; Tan NS Angiopoietin-like 4 interacts with matrix proteins to modulate wound healing. J. Biol. Chem 2010, 285, 32999–33009. [PubMed: 20729546]

(56). Chomel C; Cazes A; Faye C; Bignon M; Gomez E; Ardidie-Robouant C; Barret A; Ricard-Blum S; Muller L; Germain S; Monnot C Interaction of the coiled-coil domain with glycosaminoglycans protects angiopoietin-like 4 from proteolysis and regulates its antiangiogenic activity. FASEB J 2009, 23, 940–949. [PubMed: 19019854]

(57). Goh YY; Pal M; Chong HC; Zhu P; Tan MJ; Punugu L; Lam CRI; Yau YH; Tan CK; Huang R-L; Tan SM; Tang MBY; Ding JL; Kersten S; Tan NS Angiopoietin-like 4 interacts with integrins beta1 and beta5 to modulate keratinocyte migration. Am. J. Pathol 2010, 177, 2791–2803. [PubMed: 20952587]

(58). Choquet D; Felsenfeld DP; Sheetz MP Extracellular matrix rigidity causes strengthening of integrin-cytoskeleton linkages. Cell 1997, 88, 39–48. [PubMed: 9019403]

(59). Oka T; Xu J; Kaiser RA; Melendez J; Hambleton M; Sargent MA; Lorts A; Brunskill EW; Dorn GW; Conway SJ; Aronow BJ; Robbins J; Molkentin JD Genetic manipulation of periostin expression reveals a role in cardiac hypertrophy and ventricular remodeling. Circ. Res 2007, 101, 313–321. [PubMed: 17569887]

(60). Norris RA; Damon B; Mironov V; Kasyanov V; Ramamurthi A; Moreno-Rodriguez R; Trusk T; Potts JD; Goodwin RL; Davis J; Hoffman S; Wen X; Sugi Y; Kern CB; Mjaatvedt CH; Turner DK; Oka T; Conway SJ; Molkentin JD; Forgacs G; Markwald RR Periostin regulates collagen fibrillogenesis and the biomechanical properties of connective tissues. J. Cell. Biochem 2007, 101, 695–711. [PubMed: 17226767]

(61). Borras T; Comes N Evidence for a calcification process in the trabecular meshwork. Exp. Eye Res 2009, 88, 738–746. [PubMed: 19084518]

(62). Pohjolainen V; Rysa J; Napankangas J; Koobi P; Eraranta A; Ilves M; Serpi R; Porsti I; Ruskoaho H Left ventricular periostin gene expression is associated with fibrogenesis in experimental renal insufficiency. Nephrol. Dial. Transplant 2012, 27, 115–122. [PubMed: 21712488]

(63). Vittal V; Rose A; Gregory KE; Kelley MJ; Acott TS Changes in gene expression by trabecular meshwork cells in response to mechanical stretching. Invest. Ophthalmol. Vis. Sci 2005, 46, 2857–2868. [PubMed: 16043860]

(64). Johnson EC; Jia L; Cepurna WO; Doser TA; Morrison JC Global Changes in Optic Nerve Head Gene Expression after Exposure to Elevated Intraocular Pressure in a Rat Glaucoma Model. Invest. Ophthalmol. Vis. Sci 2007, 48, 3161–3177. [PubMed: 17591886]

(65). Didangelos A; Yin X; Mandal K; Baumert M; Jahangiri M; Mayr M Proteomics Characterization of Extracellular Space Components in the Human Aorta. Mol. Cell. Proteomics 2010, 9, 2048–2062. [PubMed: 20551380]

(66). Lyons PJ; Mattatall NR; Ro HS Modeling and functional analysis of AEBP1, a transcriptional repressor. Proteins 2006, 63, 1069–1083. [PubMed: 16538615]

(67). Layne MD; Endege WO; Jain MK; Yet S-F; Hsieh C-M; Chin MT; Perrella MA; Blanar MA; Haber E; Lee M-E Aortic Carboxypeptidase-like Protein, a Novel Protein with Discoidin and Carboxypeptidase-like Domains, Is Up-regulated during Vascular Smooth Muscle Cell Differentiation. J. Biol. Chem 1998, 273, 15654–15660. [PubMed: 9624159]

(68). Wang WH; McNatt LG; Pang IH; Millar JC; Hellberg PE; Hellberg MH; Steely HT; Rubin JS; Fingert JH; Sheffield VC; Stone EM; Clark AF Increased expression of the WNT antagonist sFRP-1 in glaucoma elevates intraocular pressure. J. Clin. Invest 2008, 118, 1056–1064. [PubMed: 18274669]

(69). Zhuo L; Hascall VC; Kimata K Inter-alpha-trypsin inhibitor, a covalent protein-glycosaminoglycan-protein complex. J. Biol. Chem 2004, 279, 38079–38082. [PubMed: 15151994]

(70). Zhuo L; Kimata K Structure and Function of Inter-α-Trypsin Inhibitor Heavy Chains. Connect. Tissue Res 2008, 49, 311–320. [PubMed: 18991084]

(71). Michaud-Levesque J; Rolland Y; Demeule M; Bertrand Y; Beliveau R Inhibition of endothelial cell movement and tubulogenesis by human recombinant soluble melanotransferrin: involvement of the u-PAR/LRP plasminolytic system. Biochim. Biophys. Acta 2005, 1743, 243–253. [PubMed: 15843038]

(72). Rolland Y; Demeule M; Beliveau R Melanotransferrin stimulates t-PA-dependent activation of plasminogen in endothelial cells leading to cell detachment. Biochim. Biophys. Acta 2006, 1763, 393–401. [PubMed: 16713448]

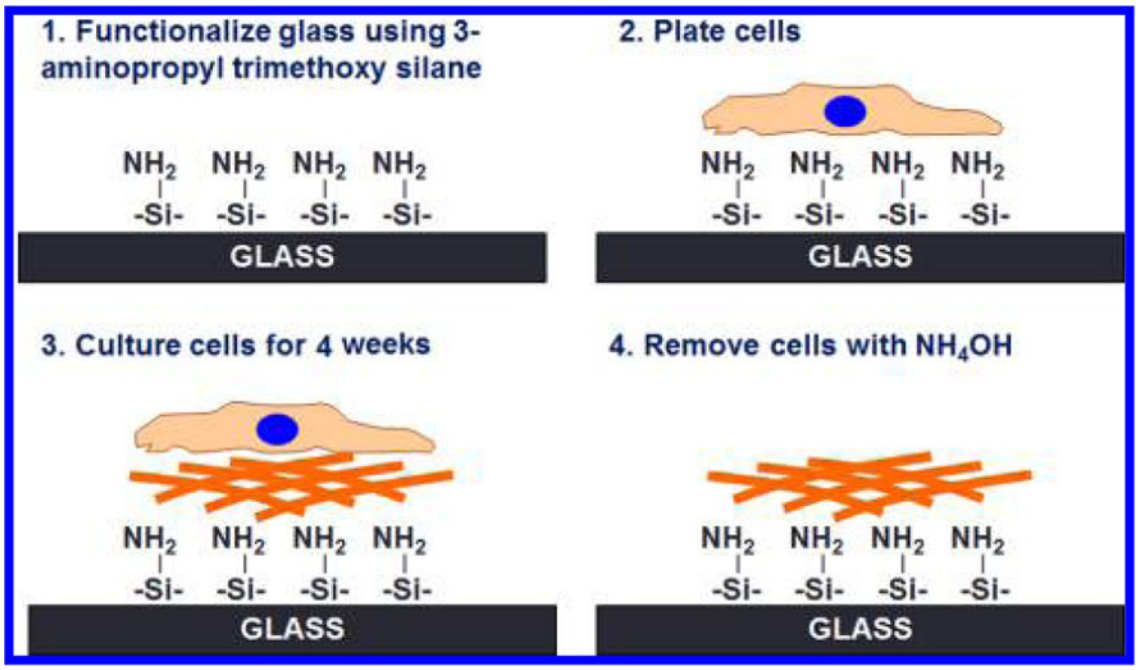

Figure 1.

Schematic illustrating the methodology to generate cell derived extracellular matrices (ECM). (A) Glass coverslips were functionalized with 3-aminopropyl trimethoxysilane. (B, C) HTM cells were cultured on silanized glass coverslips for 4 weeks either untreated or treated with 1 ng/mL TGFβ3. (D) Cultures were decellularized using ammonium hydroxide to expose the ECM deposited by cells.

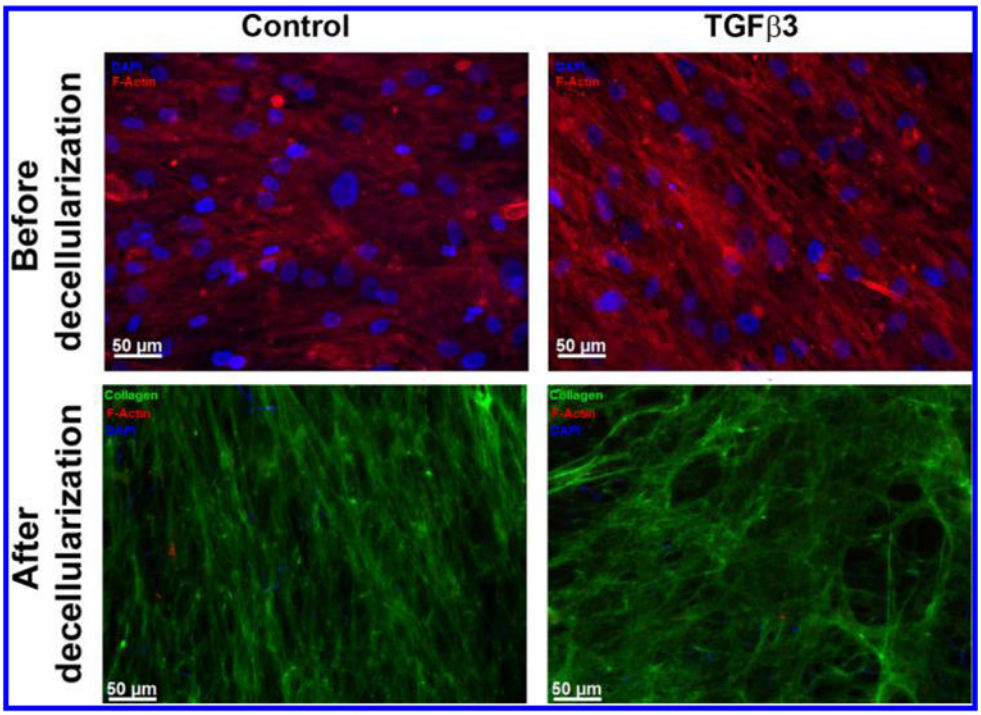

Figure 2.

Representative images of HTM cell-derived ECM from control or TGFβ3 treated cultures. Absence of staining for F-actin (Phalloidin/red) and nuclei (DAPI/blue) with abundant signal for pan-collagen immunostaining (green) demonstrated the presence of ECM devoid of HTM cells after they were removed with ammonium hydroxide. Scale bar represents 50 μm.

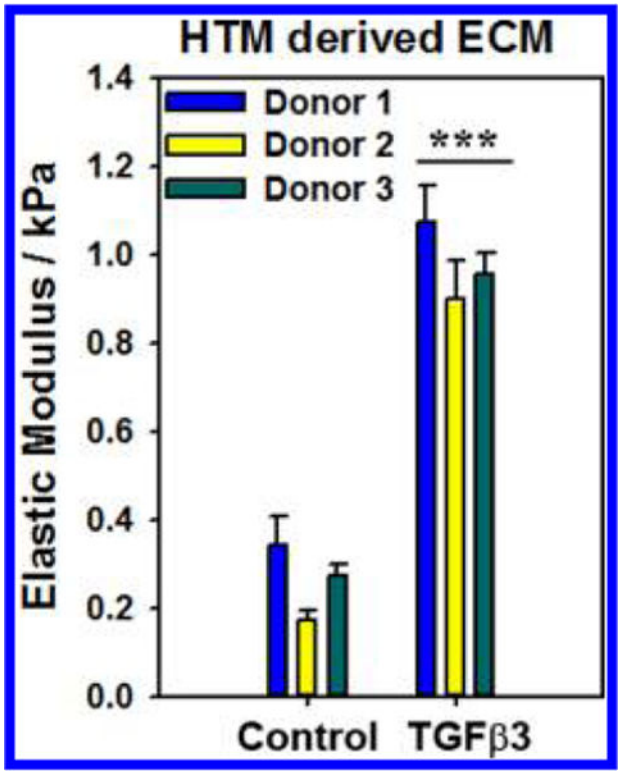

Figure 3.

Elastic modulus of ECM, measured by atomic force microscopy (AFM) using a colloidal probe (~5 μm radius), derived from TGFβ3 treated cells were significantly higher than those from control cultures. Results are mean ± standard error in mean from 7 to 10 locations, 5 force curves each location, from three donors. ***p <0.001 Mann−Whitney U-test.

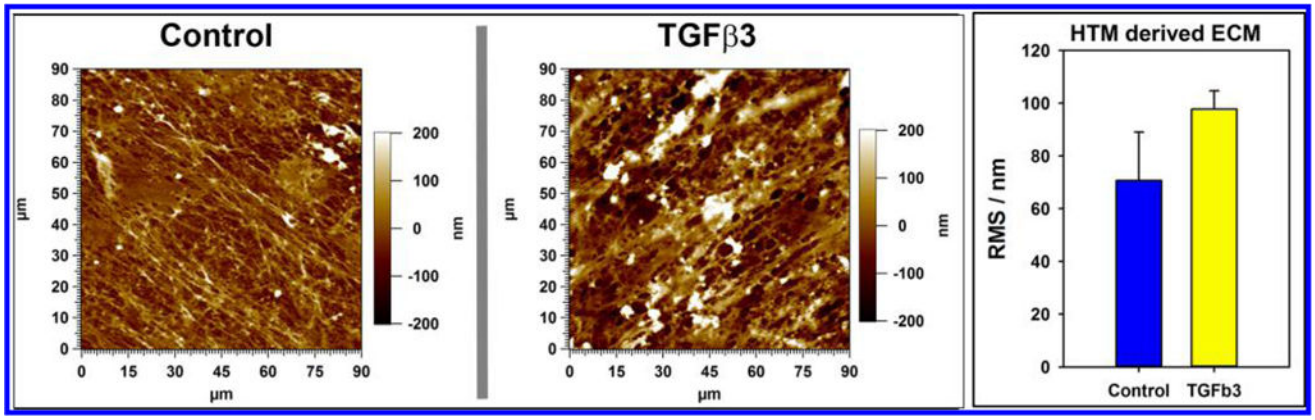

Figure 4.

Representative atomic force microscopy (AFM) images (height trace) of surface topography of ECM derived from TGFβ3-treated and control cells in contact mode in air. There were no apparent diffrerences visible between ECM obtained from either treatment. This was validated by the lack of difference observed in root-mean-square (RMS; an indicator of surface roughness) values of the ECM topography.

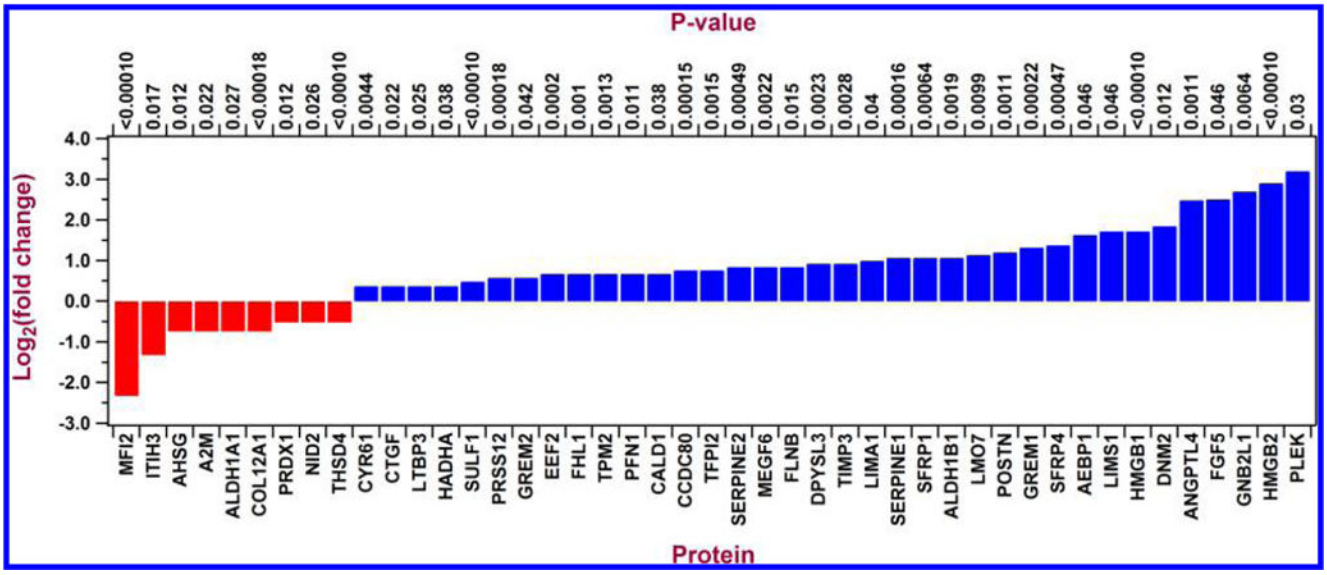

Figure 5.

Histogram illustrating log to the base 2-fold changes of ECM protein expression comparing TGFβ3 with control cultures as identified by X! Tandem LC-MS/MS. Proteins that were upregulated are in blue and those downregulated are in red comparing TGFβ3 with control cultures.

Table 1.

Gene Ontology (GO) Classification of Proteins Identified by Proteomics[a]

category	GO:TERM	genes	P-value
extracellular region	GO:0005576	FGF5, AEBP1, A2M, LTBP3, POSTN, GREM1, GREM2, TIMP3, AHSG, SERPINE2, CTGF, SERPINE1, COL12A1, ITIH3, TFPI2, PRSS12, CYR61, ANGPTL4, PLEK, MFI2, CCDC80, NID2, SFRP1, THSD4, SFRP4, SULF1, MEGF6	0.0000000001
extracellular region part	GO:0044421	FGF5, A2M, CCDC80, POSTN, NID2, GREM1, GREM2, TIMP3, AHSG, SERPINE2, SFRP1, CTGF, THSD4, SFRP4, SULF1, COL12A1, TFPI2, PRSS12, ANGPTL4	0.0000000008
Extracellular matrix	GO:0031012	CTGF, THSD4, CCDC80, COL12A1, POSTN, NID2, TFPI2, TIMP3, PRSS12, AHSG, ANGPTL4	0.0000001976
proteinaceous extracellular matrix	GO:0005578	CTGF, THSD4, CCDC80, COL12A1, POSTN, NID2, TFPI2, TIMP3, ANGPTL4	0.0000114225
extracellular space	GO:0005615	FGF5, A2M, SERPINE2, SFRP1, SULF1, SFRP4, GREM1, GREM2, AHSG, ANGPTL4	0.0004519762
extracellula matrix part	GO:0044420	CCDC80, COL12A1, NID2, TIMP3, PRSS12	0.0006823987
actin cytoskeleton	GO:0015629	PFN1, LIMA1, CALD1, TPM2, FLNB	0.0134600894
basement membrane	GO:0005604	CCDC80, NID2, TIMP3	0.0294793790

[a]Table documents the important biological functions (with greatest statistical significance for enrichment) as defined by the GO classification in the collected proteome data set of ECM from TGFβ3 treated cells that were altered at least 1.3-fold in comparison with control cultures using DAVID proteomic tool. The enrichment P-value (compared to the theoretical human proteome) is calculated based on EASE score, a modified Fisher's exact test, and ranges from 0 to 1. Fisher's Exact P-value = 0 represents perfect enrichment.

Table 2.

Gene Ontology (GO) Classification of Proteins, Altered 2-fold, Identified by Proteomics[a]

category	term	genes	P-value
extracellular region	GO:0005576	FGF5, AEBP1, PLEK, SFRP1, SFRP4, MFI2, SERPINE1, POSTN, ITIH3, GREM1, ANGPTL4	0.00006
extracellular region part	GO:0044421	FGF5, SFRP1, SFRP4, POSTN, GREM1, ANGPTL4	0.00683
extracellular space	GO:0005615	FGF5, SFRP1, SFRP4, GREM1, ANGPTL4	0.01112

[a]Table documents the important biological functions (with greatest statistical significance;cance for enrichment) as defined by GO classification in the collected proteome data set of ECM from TGFβ3-treated cells that were altered at least 2-fold in comparison with control cultures using DAVID proteomic tool. The enrichment P-value (compared to the theoretical human proteome) is calculated based on EASE score, a modified Fisher's exact test, and ranges from 0 to 1. Fisher's exact P-value = 0 represents perfect enrichment.